Electronic Supplementary Material (ESI) for Physical Chemistry Chemical Physics.

Electronic supplementary information

Molecular dynamics simulations revealed topological frustration in the binding-wrapping process of eIF4G with eIF4E

Meng Gao[1,2,3] and Yongqi Huang[1,2,3,*]

[1]Hubei Key Laboratory of Industrial Microbiology, Hubei University of Technology, Wuhan 430068, China;
[2]Cooperative Innovation Center of Industrial Fermentation (Ministry of Education & Hubei Province), Hubei University of Technology, Wuhan 430068, China;
[3]Key Laboratory of Industrial Fermentation (Ministry of Education), Hubei University of Technology, Wuhan 430068, China.

*Correspondence to: Department of Biological Engineering, Hubei University of Technology, Wuhan, Hubei, 430068 China. E-mail: yqhuang@hbut.edu.cn (Y. Huang).

Table S1. Number of binding transitions for the two types of binding pathways for $eIF4G^{391–490}$ with $eIF4E^{FL}$.

$\varepsilon_{contact}$ (wrapping)	$\varepsilon_{contact}$ (latching)	Type I	Type II
1.40	1.62	203	47
1.00	1.62	217	33
2.00	1.62	192	58
1.40	2.00	226	24
1.40	1.00	161	89
1.00	2.00	238	22
2.00	1.00	152	98

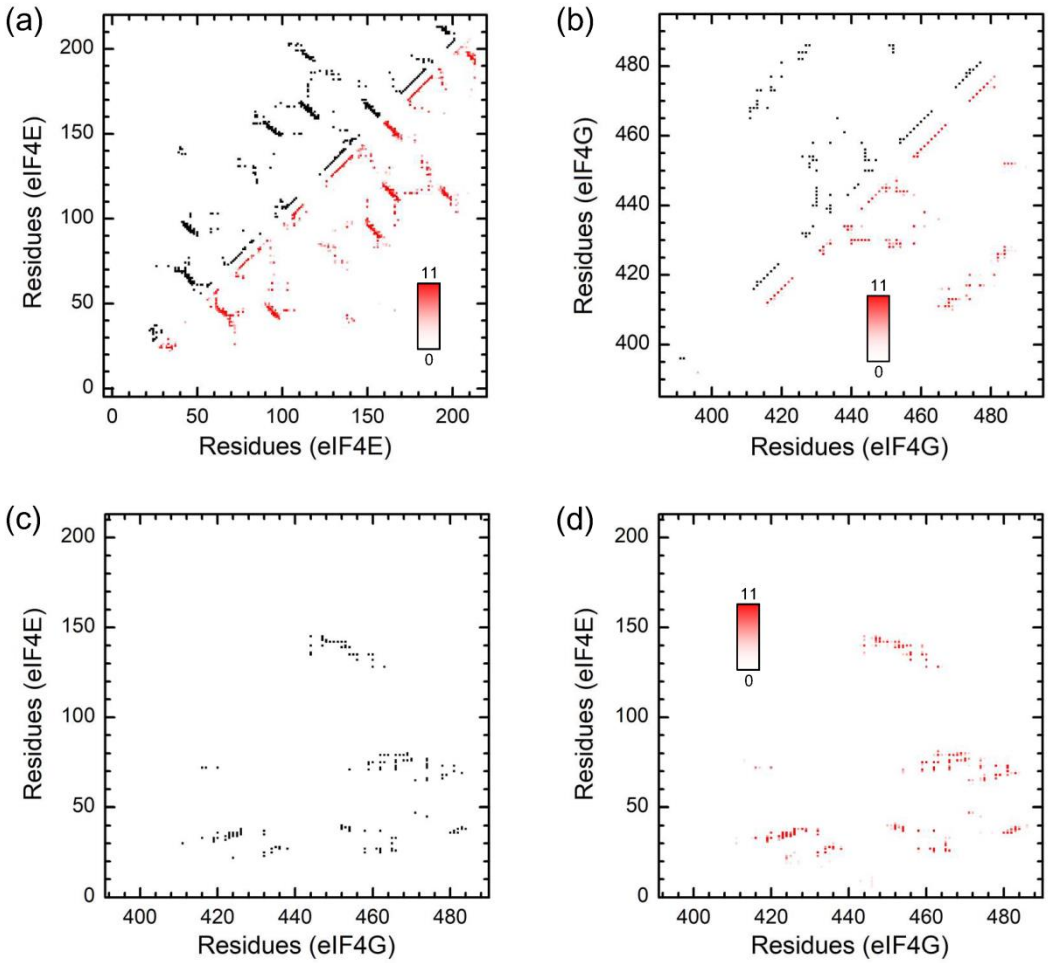

Figure S1. Native contact maps of the PDB structures of eIF4G$^{391–490}$/eIF4E^{FL} complex (PDB: 1RF8). (a) Intramolecular native contacts of eIF4E^{FL}. Top left half is the contacts formed by model 1 of the PDB structure. Bottom right half is the contacts formed by all 11 models of the PDB structure. (b) Intramolecular native contacts of eIF4G$^{391–490}$. Top left half is the contacts formed by model 1 of the PDB structure. Bottom right half is the contacts formed by all 11 models of the PDB structure. (c) Intermolecular native contacts between eIF4G$^{391–490}$ and eIF4E^{FL} formed by model 1 of the PDB structure. (d) Intermolecular native contacts between eIF4G$^{391–490}$ and eIF4E^{FL} formed by all 11 models of the PDB structure. The total number of each contact is indicated by the color bar.

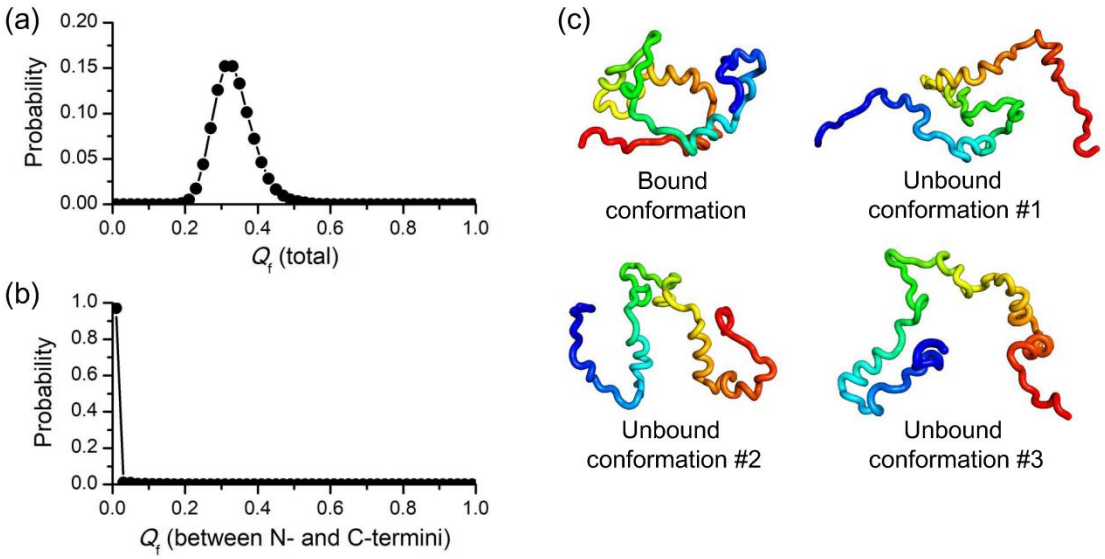

Figure S2. Analysis of MD simulations for free eIF4G$^{391–490}$. (a) Distribution of fraction of native contacts within eIF4G$^{391–490}$. (b) Distribution of fraction of native contacts between the N-terminus (residues 391−428) and the C-terminus (residues 465−490) of eIF4G$^{391–490}$. (c) Examples of conformation of eIF4G$^{391–490}$ in the unbound state. The bound conformation of eIF4G$^{391–490}$ is shown for comparison. Blue indicates the N-terminus and red indicates the C-terminus.

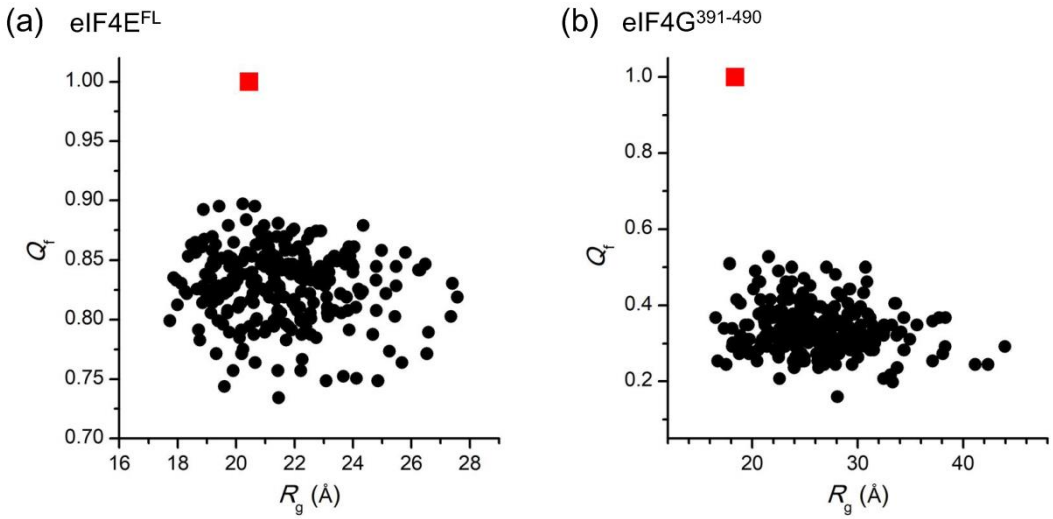

Figure S3. Properties of 250 initial conformations for binding simulations. (a) Fraction of native contacts and radius of gyration for eIF4E^{FL}. (b) Fraction of native contacts and radius of gyration for eIF4G$^{391–490}$. Values corresponding to the NMR structure were indicated in red squares.

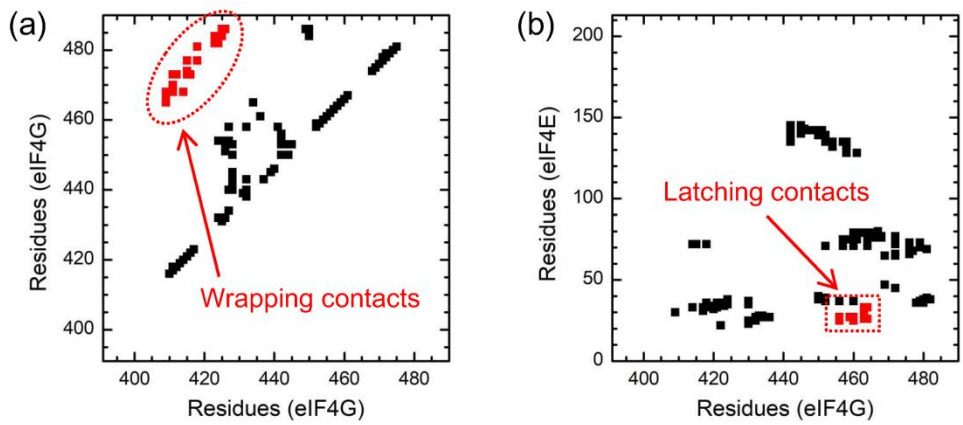

Figure S4. Identification of wrapping contacts and latching contacts. (a) Intramolecular native contacts of eIF4G$^{391–490}$ in the eIF4G$^{391–490}$/eIF4E^{FL} complex. The wrapping contacts are indicated in red. (b) Intermolecular native contacts between eIF4G$^{391–490}$ and eIF4E^{FL} in the eIF4G$^{391–490}$/eIF4E^{FL} complex. The latching contacts are indicated in red.

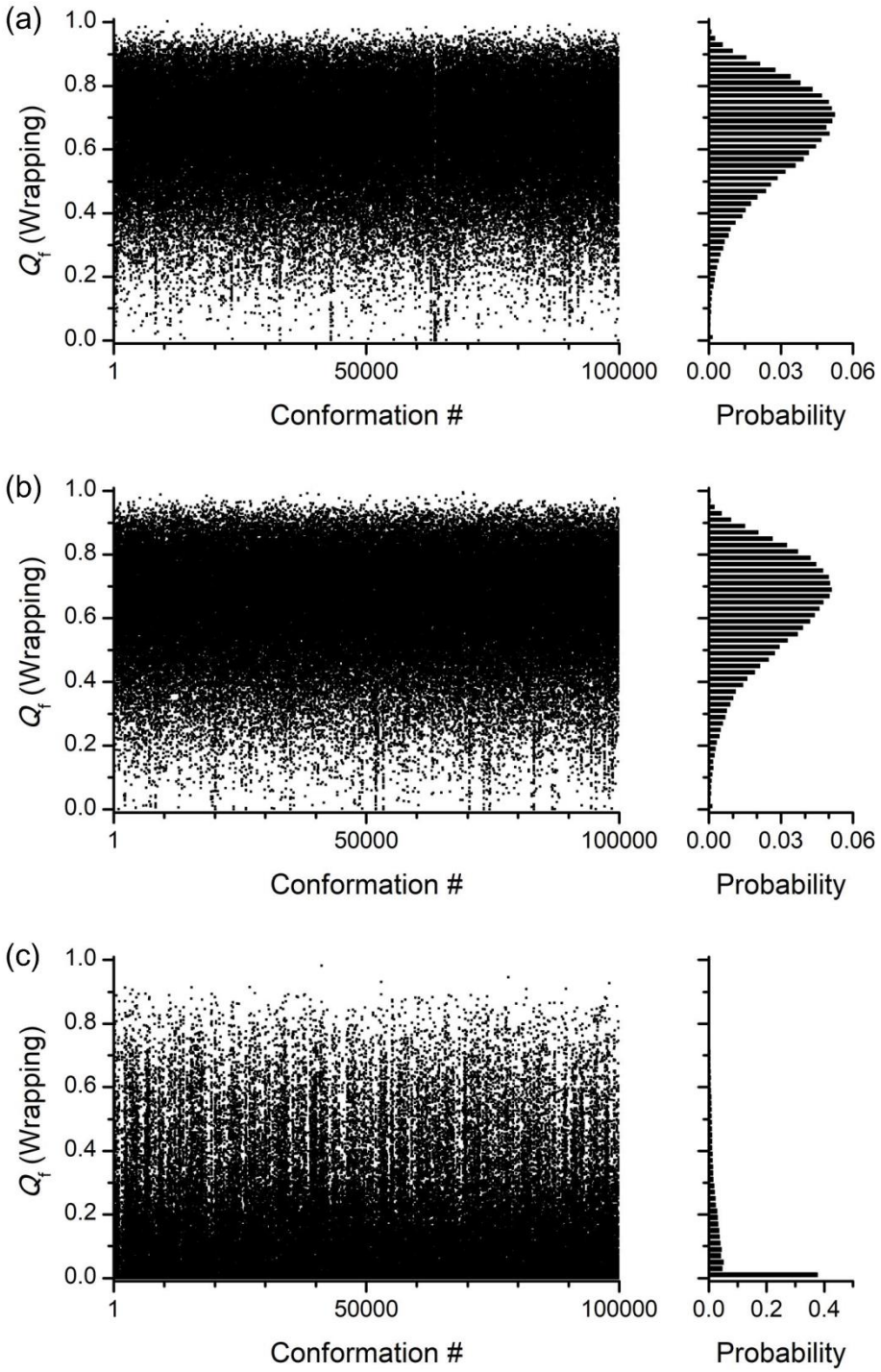

Figure S5. Wrapping contacts were analyzed for 100000 conformations of eIF4G$^{391–490}$ bound to eIF4E^{FL} (a), eIF4E$^{\Delta 20}$ (b), and eIF4E$^{\Delta 35}$ (c). In this analysis, we focused on the conformations of eIF4G bound to eIF4E. Therefore, we applied stronger intermolecular contacts ($\varepsilon_{contact}$ = 2.5 ε) between residues 452−458 of eIF4G (the canonical eIF4E-binding motif) and eIF4E to avoid unbinding. $\varepsilon_{contact}$ for other intermolecular contacts was set to 1.62 ε. MD simulations with 2×10^8 steps were performed using the complex states as initial conformations and trajectories were saved every 1000 steps. The last half trajectories were analyzed.

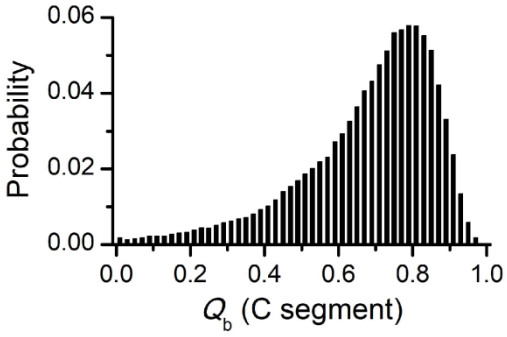

Figure S6. Distribution of fraction of intermolecular native contacts between the C-terminal segment (residues 366–490) of eIF4G$^{391–490}$ and eIF4E$^{\Delta35}$ analyzed from 100000 conformations of eIF4G$^{391–490}$ bound to eIF4E$^{\Delta35}$ obtained from simulations indicated in Figure S5.

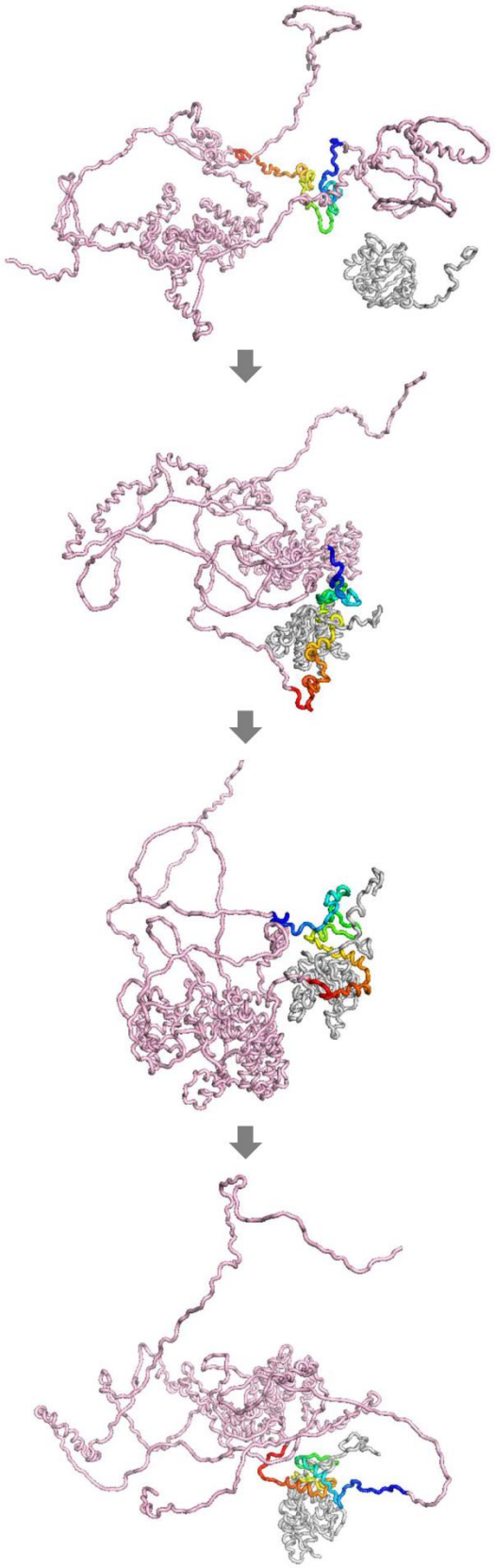

Figure S7. Examples of conformations of eIF4G^{FL} and eIF4E^{FL} along a binding trajectory. eIF4G^{FL} is shown in light magenta with the eIF4E-binding domain of eIF4G^{FL} indicated in rainbow color. eIF4E^{FL} is shown in gray.